Soft Matter

Accepted Manuscript

ROYAL SOCIETY OF CHEMISTRY

www.rsc.org/softmatter

Gelation of large hard particles with short-range attraction induced by bridging of small soft microgels

Junhua Luo,[a,b] *Guangcui Yuan*,*[,a] *Chuanzhuang Zhao*,[c] *Charles. C. Han*[*,a]

Jie Chen,[d] and *Yun Liu*[de]

[a] State Key Laboratory of Polymer Physics and Chemistry, Joint Laboratory of Polymer Science and Materials, Beijing National Laboratory for Molecular Sciences, Institute of Chemistry, CAS, Beijing 100190, China;

[b] University of Chinese Academy of Sciences, Beijing 100049, China;

[c] Department of Polymer Science and Engineering, Faculty of Materials Science and Chemical Engineering, Ningbo University, Ningbo 315211, P. R. China;

[d] Center for Neutron Research, National Institute of Standards and Technology, Gaithersburg, Maryland 20899, USA;

[e] Department of Chemical and Biomolecular Engineering, University of Delaware, Newark, Delaware 19716, USA.

Corresponding authors: Guangcui Yuan (E-mail: gcyuan@iccas.ac.cn) and Charles C. Han (E-mail: c.c.han@iccas.ac.cn)

Telephone: +86 10 82618089. Fax: +86 62521519

Abstract

In this study, mixed suspensions of large hard polystyrene microsphere and small soft poly(N-isopropylacrylamide) microgel is used as model systems to investigate the static and viscoelastic properties of suspensions which go through liquid to gel transitions. The microgels cause short-range attraction between microspheres through bridging and depletion mechanism whose strength can be tuned by the microgel concentration. Rheological measurements are performed on suspensions with the volume fraction (Φ) of microsphere ranging from 0.02 to 0.15, and the transitions from liquid-like to solid-like behaviors triggered by the concentration of microgels are carefully identified. Two gel lines due to bridging attraction under unsaturated conditions are obtained. Ultra-small angle neutron scattering is used to probe the thermodynamic properties of suspensions approaching to the liquid-solid transitions. Baxter's sticky hard-sphere model is used to extract the effective inter-microsphere interaction introduced by the small soft microgels. It is found that the strength of attraction (characterized by a single stickiness parameter τ) on two gel lines formed by bridging are very close to the theoretical value for spinodal line in the τ - Φ phase diagram predicted by Baxter's model. This indicates that the nature of gel state may have the same thermodynamic origins, independent of the detailed mechanism of the short-range attraction. The relationship between the rheological criterion for the liquid-solid transition and the thermodynamic criterion for the equilibrium-nonequilibrium transition is also discussed.

1. Introduction

The nature of gelation in short-range attractive colloidal systems where the interparticle potential has a range significantly smaller than the colloidal size, has received significant attention in recent years.[1-3] Various routes to gel state have been proposed, including the out of equilibrium route such as diffusion-limiting cluster aggregation (DLCA) models in the limit of very strong attraction,[4-6] the non-equilibrium route such as arrested phase separation,[7-10] and the equilibrium route that the gel line can be more stable than the coexistence curve.[11, 12] DLCA route has been known as purely kinetic process that fractal clusters grow irreversibly due to strong attraction and ultimately interconnect to create a space-spanning network even at very low colloid volume fraction (Φ). Controversial problems remain for systems with a finite strength of attraction (U) of $\lesssim 10\,k_{\mathrm{B}}T$ (k_{B} is the Boltzmann's constant, and T is the temperature), where the system may undergo a liquid-gas phase separation that intervenes with dynamical arrest. The relative position of the gel line and the liquid-gas coexistence line in the U-Φ plane, in another words, how percolation interferes with phase separation, is closely related to a central question of recent research in colloidal science that, whether colloidal gel can be described in a colloidal glass framework invoked by mode coupling theory.[13,14]

Various systems, such as charge stabilized colloidal particles with added electrolyte,[15-17] colloidal particle coated with thermal sensitive surface layer,[18, 19] and protein,[10] *et al.* have been used to study the gelation behavior of attractive colloids. But the most widely used model systems are mixed suspensions of colloid and

non-adsorbing polymer with a depletion attraction. A notable example is sterically stabilized poly(methylmethacrylate) particles suspended in organic media with polystyrene as depleting agent.[7-9, 20, 21] The range and the depth of depletion potential can be easily adjusted by, respectively, the size ratio and the free volume concentration of non-adsorbing plymer.[22, 23]

Addition of a small amount absorbing polymer to colloidal dispersions can also lead to aggregation or gelation. The gelation mechanism at molecular level, either by bridging or depletion, depends on whether the added polymer is adsorbing or non-adsorbing.[24] The interpretations of bridging mechanism and depletion mechanism are distinct, where the former gets its name from the direct link or "bridge" between neighboring particles in the aggregates, and the latter from the fact that the region between the neighboring particles is "depleted" of polymer.[25-27] Compared to the widely-used depletion attraction, sticking of two particles by bridging also corresponds to a short-range attractive interaction between the two particles if the radius of gyration of added polymer is smaller than the colloidal size. Theoretical models[28, 29] and direct measurements[30-32] show that, for attractive interaction induced by bridging polymer in inter-surface gap, the range is in the order of radius of gyration of added polymer and the strength is very sensitive to surface coverage. Therefore, in statistical-mechanical approach, the inter-particle potential in mixed suspension of colloids either with adsorbing polymers or with non-adsorbing polymers can be treated in the same model, such as the Baxter's[33] sticky hard-sphere potential. For example, Dickinson[25-27] mapped out the equilibrium gelation behavior

in concentrated dispersion either by bridging flocculation or by depletion flocculation with the same statistical model based on the Baxter's[33] approach. The Baxter's[33] model, with a rather unphysical infinitely deep potential at close contact, is a relatively simplified model, but it correctly predicts the essential features of a sticky hard-sphere system.[34] The Baxter's[33] approach to the adhesive system has the advantage that the phase diagram including the spinodal[35] and the dynamic percolation[36] can be determined analytically. Experimentally, the effective interaction between colloid can be extracted from scattering data with a structure factor model based on Baxter's[33] potential. For example, by using small-angle X-ray scattering, Bharti *et al.*[37] investigated the influence of PH, ionic strength and protein concentration on the effective interaction between silica particles caused by protein bridging.

Although bridging is a direct way to stick colloids which leads to gel formation, the systems with bridging attraction are rarely taken as model colloidal systems in the investigation of gelation behaviors of colloids with short-range attraction. The bridging flocculation is often taken as a purely kinetics-controlled process. A well known characteristic of polymers which induced bridging flocculation is that the system tends to become re-stabilized at high polymer concentration as the particle surfaces become fully saturated at the monolayer level by the adsorbing polymeric species. In another words, for given volume fraction of colloid, a liquid-gel-liquid transition will be obtained with increasing concentration of adsorbing polymers. Therefore, there shall be two gelation boundaries due to bridging mechanism. The

existing theories of bridging flocculation are based on the well-known kinetic model of La Mer[38, 39], with a factor $\theta(1-\theta)$ being roughly used to evaluate the efficiency and sensibility for irreversible binary collisions between the primary particles. Here, θ is surface coverage which measures the fraction of surface of the colloid particle covered by the adsorbed polymer.

In this study, we use mixed suspensions of large hard microsphere and small soft microgel as model systems to investigate the thermodynamic and viscoelastic properties of suspensions which approach the liquid-gel-liquid transitions through bridging and steric stabilized mechanisms. Small poly (N-isopropylacrylamide) (PNIPAM) microgels are absorbable to the surface of large polystyrene (PS) microspheres. For a given volume fraction of PS microspheres (Φ_{MS}), with increasing concentration of microgel (Φ_{MG}), the stabilizing bare microspheres first aggregate with each other through the bridging of microgels, then disperse individually when saturated adsorption is achieved. The rheological, microscopic and light scattering characterizations of the aggregation, gelation and glass transition of this mixing system has been reported in our previous publications.[40, 41, 61] The dosage of microgels is an important factor in triggering the aggregation and stabilization of microspheres. In this study, small-amplitude oscillatory shear rheological measurements are performed on suspensions with Φ_{MS} ranging from 0.02 to 0.15, and the transitions between liquid-like and solid-like behaviors triggered by Φ_{MG} are carefully identified. The gelation boundaries, due to bridging attraction under unsaturated conditions, are identified.

Previous experimental[42, 43] and theoretical[44, 45] works have shown that the precise shape of the attractive part of the interaction potential appears to be rather unimportant for thermodynamic phase diagrams provided that the range of attraction interaction is significantly short compared to the size of colloid particles. Moreover, when the strength of attraction in terms of stickiness τ or normalized second virial coefficient B_2* (τ and B_2* are related with each other) is used as control parameter, at a given value of stickiness, not only the thermodynamic properties such as inter-particle structure factor $S(q)$ (q is the scattering vector) but also dynamics are identical for potentials with different range of square-well attraction.[1,46] Therefore, in the present study, Baxter's sticky hard-sphere potential will be used to understand the data from Ultra-small Angle Neutron Scattering (USANS) and investigate the microstructure of the dispersions at and around the gelation boundaries given by rheological measurements. Quantitative modeling of the USANS scattering profile with Baxter's potential yields the strength of attraction in terms of stickiness τ. Combining with the τ - Φ phase diagram derived from Baxter's potential,[33-36] we compare the thermodynamic properties of the dispersions approaching to the gelation boundaries. Our aim is to build a model system with short-range attraction coming from the clearly well-defined bridging interaction and to find out the nature of gel state in short-range attractive colloidal systems.

2. Experimental Section

2.1 Materials and Sample Preparation

The preparation method of mixed colloidal system used in the current experiments was previously described.[40, 41] The PS microspheres were synthesized through a one-stage dispersion polymerization. The radius of gyration (R_g) of PS microspheres determined by USANS is 1023 nm. The hydrodynamic radius (R_h) of PS microspheres determined by dynamic light scattering (ALV/DLS/SLS-5022F) is about 1300 nm and the polydispersity index is about 1.06. The bulk density of polystyrene (ρ = 1.05g/cm^3) is used to calculated Φ_{MS}. The PNIPAM microgels were synthesized according to the procedure of Senff and Richtering.[47] The R_h of PNIPAM microgels is determined to be 130 nm at 20 ^oC by dynamic light scattering (ALV/DLS/SLS-5022F). The effective Φ_{MG} in its dilute dispersion is estimated from viscosity measurements via Bachelor[48] expression :

$$\eta_0/\eta_s = 1+2.5\Phi_{eff}+5.9\Phi_{eff}^2 , \quad (1)$$

Where η_0 and η_s is the viscosity values of the microgel dispersion and the solvent, respectively, and Φ_{eff} is the effective volume fraction. To determined $\Phi_{MG,}$ we assumed that the swelled microgel particles could be modelled as hard spheres in dilute suspension and we have $\Phi_{MG} = \Phi_{eff}$. Actually, the actual volume fraction of PNIPAM microgel is changed when mixing with PS microspheres due to adsorption and deformation, but Φ_{MG} estimated from the hard sphere approxmation is still used as a measure of the dosage of PNIPAM microgel in mixed suspensions in the present study, which will not affect the discussion. The mixed suspensions of PS microsphere and PNIPAM microgel are homogenized by ultrasonic wave at 20^oC for 60 minutes after mixing.

2.2 Rheology

Rheological properties of the dispersions were investigated by a stress-controlled rheometer (Anton Paar MCR 501) with a 25 mm cone-plate geometry. Silicon oil was coated on the edge of the cone-plate sample cell to prevent the evaporation of solvent. As a standard protocol, a high strain dynamic shear rejuvenation (γ_0 = 1000%, ω = 1 rad/s) was performed followed by a waiting time of typical 30 minutes before each experiment. Waiting time of 30 minutes was chose to assure that the viscoelastic properties did not change and reproducible results were obtained in consecutive tests. The oscillation strain sweep measurements were performed at constant frequency of ω = 1 rad/s. The maximum stress during the strain sweep was recorded. Temperature was kept at 20 ^{o}C during the rheological measurement.

2.3 Ultrasmall-Angle Neutron Scattering (USANS).

USANS measurements were carried out at the U.S. National Institute of Standards and Technology (NIST) on the BT5 perfect crystal diffractometer. By using a neutron wavelength of 2.4 Å (6% $\Delta\lambda/\lambda$), a q-range of 0.00003-0.0026 Å^{-1} was accessed.[49] Samples were loaded into demountable titanium cells with a 1 mm path length. The data were reduced to absolute scale and analyzed with the NIST-provided algorithms for WaveMetrics Igor Pro software.[50]

The application of small-angle neutron scattering or x-ray scattering to investigate the structure of polymer-flocculated monodispersed particles has been reported.[37, 51, 52] The technique is based on the fact that the interference pattern of the scattered radiation is determined by the distribution of the separations between particle centers

in the flocs. Scattering from colloidal dispersions results from the difference in the scattering length density (*SLD*) between the particles and the surrounding medium. Scattering from the adsorbing species makes a negligible contribution.[24] In the present system we have two types of particles, *viz*. PS microspheres and PNIPAM microgels. But scattering intensity is dominated by the PS microspheres due to their larger size and higher neutron scattering contrast against the medium compared to the PNIPAM microgels. The scattering from the microgels bound to the PS microsphere or dispersed in the solvent can be neglected during data analysis. Hence, our USANS data can be analyzed by the formalism for one-component particle dispersions. The effects caused by the PNIPAM microgels are indirectly incorporated into their influence on the effective interaction between the PS microspheres. To avoid the sedimentation of PS microspheres, a buoyancy-matching mixture of H_2O and D_2O with equal volume was used as the solvent in the present study.

The absolute coherent neutron scattering intensity can be modeled as

$$I(q) = \Delta\rho^2 \Phi_P V_P P(q) S(q), \quad (2)$$

where $\Delta\rho$ is the difference in *SLD* between the particles and the solvent/matrix, Φ_P is the volume fraction of particles (here PS microsphere), V_P is the volume per particle, $P(q)$ and $S(q)$ are form factor and inter-particle structure factor describing the contribution to the scattering intensity from a single microsphere and the interference from the spatial arrangement of microspheres, respectively. Here, the PS microspheres are modeled using a monodisperse sphere form factor. $S(q)$ is calculated using the Ornstein−Zernike[53] (OZ) equation with the Percus−Yevick[54] (PY)

closure approximation scaled by the mean particle diameter.

An analytical solution to the OZ equation with the PY closure approximation for an adhesive pair potential was obtained by Baxter[33] with a pair-wise potential defined as

$$V(r) = \lim_{\Delta \to 0} \begin{cases} \infty & r < \sigma \\ k_B T \ln\left[12\tau\left(\frac{\Delta}{\sigma+\Delta}\right)\right] & \sigma \le r \le \sigma + \Delta \\ 0 & r > \sigma + \Delta \end{cases}, \quad (3)$$

where Δ represents the width of the square well, σ is the hard-core particle diameter. The range of attraction, characterized by a perturbation parameter $\varepsilon = [\Delta/(\sigma+\Delta)]$, should be held less than 0.1.[45] Within the framework of this model, the strength of attraction is characterized by a single interaction parameter τ (stickiness parameter), which is a dimensionless indicator of the temperature. The quantity τ^{-1} is a measure of stickiness of the particles, with $\tau^{-1} \to 0$ corresponding to non-sticky hard sphere. τ is related to the reduced second virial coefficient B_2^* by

$$\tau = \frac{1}{4(1-B_2^*)}. \quad (4)$$

The pair-interaction potential of our system can be modelled with the Baxter's[33] potential since the size of the PNIPAM microgel is very small in comparison to the size of the PS microsphere. The fitting of scattering intensity includes 7 parameters: volume fraction (Φ_{MS}), radius of sphere (R_g = 10230 Å), *SLD* of sphere (1.4×10^{-6} Å^{-2}), *SLD* of solvent (2.9×10^{-6} Å^{-2}), perturbation parameter (ε), stickiness (τ) and background. The first 4 parameter are acquired from independent experiments. For the fitting of the perturbation parameter using Baxter's sticky hard-sphere Model, it uses

the limiting case where the range of attraction approaches zero. The background is obtained from the asymptotic value at large q as the scattering intensity is expected to follow the Porod law. Therefore, the stickiness is in fact the only unconstrained variable in the fitting.

3. Results and Discussion

3.1 Bridging and Depletion

In our previous study,[40,41] we have visually observed the effects of Φ_{MG} on the clustering and stabilization behaviour of particles by using optical microscopy. A schematic illustration of clustering (or gelation) of the PS microsphere with increasing Φ_{MG} has been proposed in our previous publication.[41] For the readers' convenience, we reuse the schematic diagram in the current paper as Figure 1. (a) With the absence of PNIPAM microgels, PS microspheres are homogeneously dispersive in the suspension. The stability of PS microspheres is provided by a very thin (about 18 nm) poly(vinylpyrrolidone) (PVP) layer, which is non-charged and water-soluble, covalently bonded to the surface of PS microspheres. (b) With the addition of a small amount of microgels, clusters form, and they grow dramatically with a little more microgels. The absorption of PNIPAM microgels to the surface of PS microsphere is confirmed by dynamic light scattering, whose results show that the R_h of microsphere with addition of microgels is larger than that without the addition of microgels.[41] The unambiguous bridging of microgels is also confirmed by scanning electron microscopic observation of lyophilized mixed suspension in which the microsphere

surface is partially covered by some flaky microgels and the gap between microspheres is connected by microgels. (c) When Φ_{MG} increases to a certain value, the large clusters dissolve and the visible particles are completely dispersed. The stability of PS microspheres under this condition is provided by the adsorbed microgels which fully covered the surface of PS microspheres and played the role of a stabilizer. (d) With further increase of Φ_{MG} to an over-saturated state, clusters re-appear. The reason has been taken as depletion attraction.

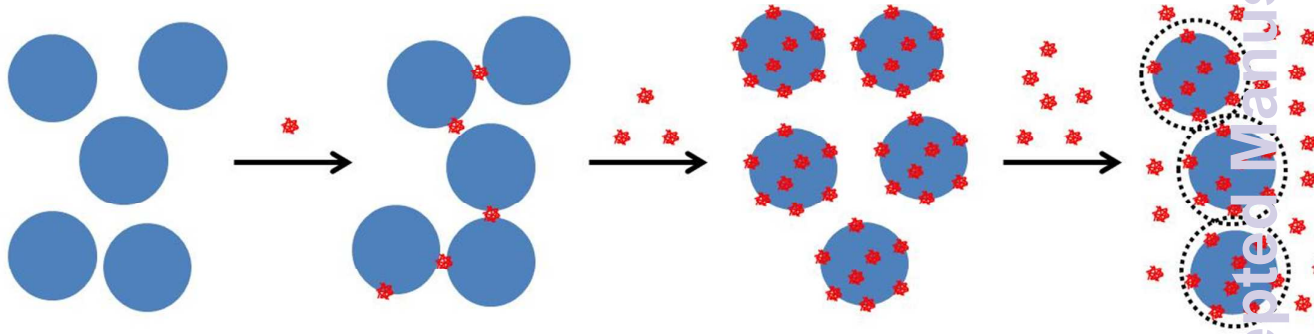

Figure 1 A schematic illustration of clustering (or gelation) of the PS microsphere with increasing concentration of PNIPAM microgel (Φ_{MG}), reprinted from Figure 9 of our previous paper.[41] The microsphere and microgel are presented by blue circle and red circle, respectively. The microsphere, microgel and depletion layer is presented by blue circle, red circle and dotted circle, respectively.

It is known that when the net particle–polymer (here microgel) interaction is weak, the bridging and depletion types of flocculation are reversible, and a small change in the condition of solution may cause a substantial change in the equilibrium extent of flocculation, or even in the type of flocculation.[24, 27] PNIPAM is considered as a typical water-soluble polymer which bears both hydrophilic (amide) and hydrophobic

(isopropyl and the backbone) groups. The driving force for adsorption of PNIPAM microgel to the surface of PS microsphere coated with a very thin PVP layer is considered to be hydrophobic interaction. The critical adsorption free energy needed for polymer adsorption is relatively low, of the order of $0.3k_BT$ per segment,[59] and the hydrophobic interaction between PNIPAM microgel and PS microsphere shall satisfy this requirement. With the addition of a small amount of microgel, adsorption of PNIPAM microgel to PS microsphere surface occurs on condition that the adsorption free energy is able to compensate for the configurational entropy loss which occurs on transfer of PNIPAM microgel from solution to an interface. The adsorption and bridging mechanism for this specific system has been discussed in our previous work.[40] It has been found that the adsorption of a free microgel to one microsphere surface is very fast with relatively negligible desorption, but the connection of the adsorbed microgel to another microsphere surface is a reversible process. It should be emphasized that the reversible bridge formation and disconnection process is very important because of the following two factors. First, it is the essential prerequisite for structure or state transition tuned by Φ_{MG} for this specific system. Second, it provides us the possibility to apply Baxter's theory to the bridging system, at least for the case with $\theta \to 0$ or $(1-\theta) \to 0$, because Baxter's model describes the equilibrium properties and structure. Generally, irreversible adsorption originates from the multiple anchoring points on the microsphere surface, because desorption of a microgel requires a simultaneous release of all anchoring points and a fast diffusion of the microgel away from the particle surface. With the increasing amount of microgels

until the volume fractions of small and large particles are comparable, there will be many more small particles than large particles, and the small spheres will provide the dominant contribution to the free energy (and entropy) of the system. The entropy-driven depletion effect will produces an effective attraction potential between large particles with the well depth being approximately proportional to the volume fraction of free small particles.

The effective inter-microsphere interaction during the stabilization → flocculation → re-stabilization → flocculation process triggered by Φ_{MG} is characterized by USANS. Fig. 2(a) gives the absolute scattering intensity $I(q)$ obtained from relatively dilute dispersions of PS microspheres (Φ_{MS} = 0.02) without and with four different concentrations of PNIPAM microgels. As a comparison, the scattering data (star symbols) for a dispersion of PNIPAM microgels with Φ_{MG} = 0.14 (which is much higher than that used in mixed suspensions) is also provided. The scattering contribution of PNIPAM microgels is found to be smaller than that of PS microspheres by nearly a factor of 1000. Therefore, it is clear that the scattering is dominated by PS microsphere. As a matter of fact, at high q value ($q > 3.0 \times 10^{-4}$ Å^{-1}, $qR > 3.0$) where the main feature is the shape of the particles, all scattering curves from mixed suspensions are in agreement with that of PS microsphere suspension without PNIPAM microgels. At intermediate q region ($8.0 \times 10^{-5} < q < 3.0 \times 10^{-4}$ Å^{-1}), where the interferences are determined by the correlation of the centers of PS particles, no noticeable peak is found for all curves, which is clearly different with those colloidal systems with strong long range repulsion.[19, 37, 51, 52] The absence of peak and

depression in this length scale indicates that there is no preferred distance between PS microsphere. At low q values ($q < 8.0 \times 10^{-5}$ Å^{-1}) which correspond to distances larger than the dimensions of the individual particles or the separations between them, the scattering curves for mixed suspensions (except the one with $\Phi_{MG}/\Phi_{MS} = 1.9 \times 10^{-2}$) resemble that of bare PS microsphere that $I(q)$ approaches a constant limiting value， indicating a stable colloidal dispersion or no existence of macroscopic flocs. At least, most microspheres remain free even when clusters exist. While for sample with $\Phi_{MG}/\Phi_{MS} = 1.9 \times 10^{-2}$, there is considerable rise in the intensity toward $q \rightarrow 0$ limit indicating that this colloidal liquid is trapped into a structure which is heterogeneous at large length scales. The real space photographs in the inset of Fig. 2(a) show that the mixed suspension with $\Phi_{MG}/\Phi_{MS} = 1.9 \times 10^{-2}$ is clearly split into a colloidal-poor phase and a colloidal-rich phase.

Fig. 2b is an expanded view of the scattering curves at intermediate q region ($8.0 \times 10^{-5} < q < 3.0 \times 10^{-4}$ Å^{-1}). Within experimental accuracy, the scattering curve from sample with $\Phi_{MG}/\Phi_{MS} = 0.26$ is almost identical with that of bare PS microsphere dispersion, and the scattering curve from sample with $\Phi_{MG}/\Phi_{MS} = 1.43$ is almost identical with that with $\Phi_{MG}/\Phi_{MS} = 4.3 \times 10^{-3}$. It should be noted that the Baxter's[33] model provides analytical solution only for equilibrium dispersion.[55] There are no physical acceptable solutions of the PY equation for systems inside the unstable region, or in other words, for systems with stickiness parameter below a boundary value (τ_B). The boundary values as function of particle volume fraction are provided in ref. 35. The green solid curve in Fig.2(a) and Fig.2(b) corresponds to the theoretical

calculation of intensity using the boundary value ($\tau_B = 0.064$, $B_2^* = -3.2$) for Φ_{MS} = 0.02 below which there is no analytical solutions for the scattering curve. For sample with $\Phi_{MG}/\Phi_{MS} = 1.9 \times 10^{-2}$, the intensity rise in the low q region appears to follow a power law with $I(q) \propto q^{-1.2}$, the typical characteristic of a kinetic arrested process. As a consequence, it is impossible to fit the entire q range with Baxter's model for sample with $\Phi_{MG}/\Phi_{MS} = 1.9 \times 10^{-2}$. While for other curves in Fig. 2(a), fits of the $I(q)$ curves show good agreement throughout the entire q-range. The fitting parameters τ are showed in the legends of Fig. 2(b) and the corresponding analyzed B_2^* values are plotted in Fig. 2(c). The open square in Fig. 2(c) corresponds to the boundary value for Φ_{MS} = 0.02. For reference, $B_2^* = 1$ and $B_2^* = 0$ corresponds to a hard sphere fluid and the definition of the Boyle temperature, respectively. This result is consistent with the microscopical observation discussed above, i.e., the suspensions experienced a stabilization → flocculation → re-stabilization → flocculation transition process with increasing Φ_{MG}.

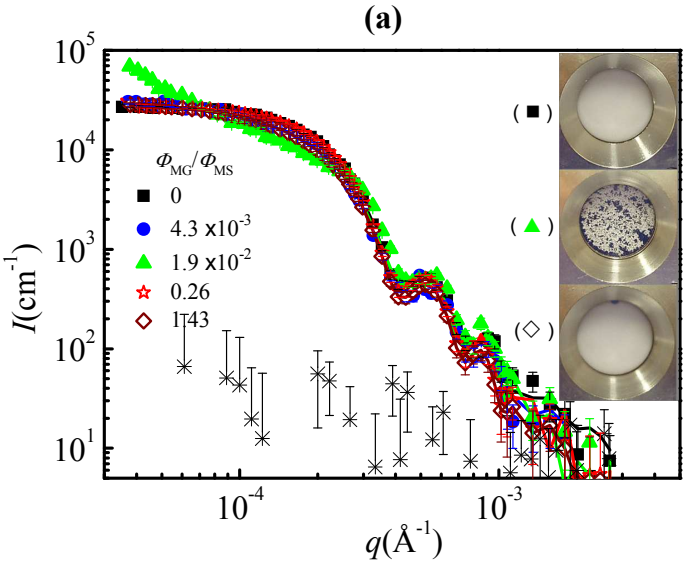

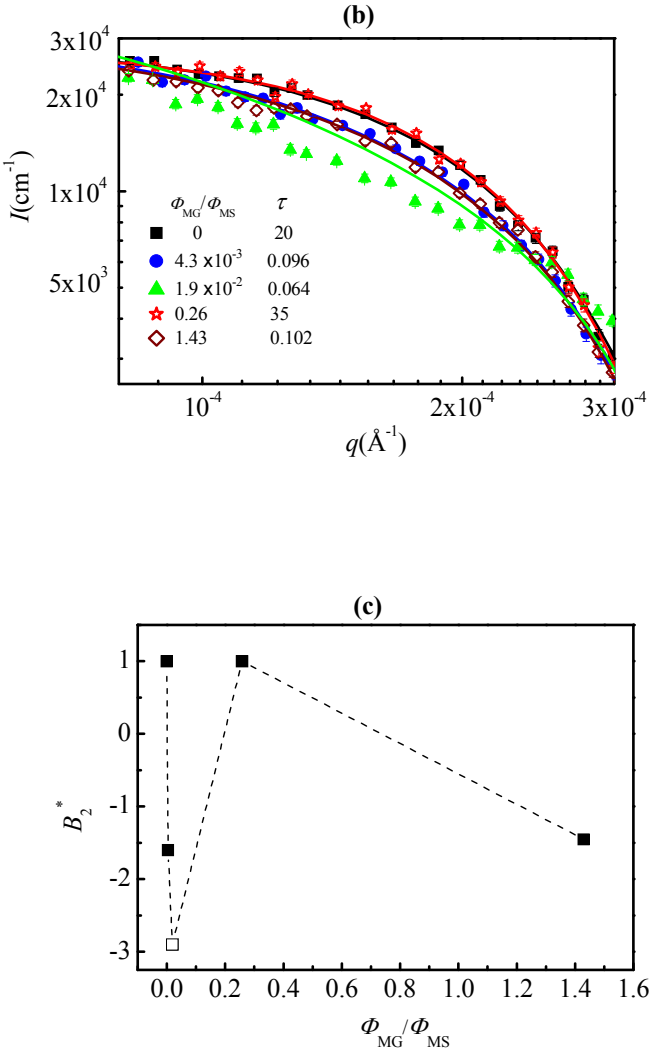

Figure 2 (a) Experimental (symbols) and fit (solid lines) intensity data scattered from suspensions with Φ_{MS} = 0.02. The scattering data (✳) from dispersion of pure PNIPAM microgel (Φ_{MG} = 0.14) is also provided. Inset is corresponding pictures of samples with widow diameter of 1 inch. **(b)** An expanded view of the scattering curves at intermediate q region ($8.0 \times 10^{-5} < q < 3.0 \times 10^{-4}$ Å^{-1}). **(c)** The corresponding reduced second virial coefficient B_2^* vs. mixing ratio (Φ_{MG}/Φ_{MS}).

3.2 Rheological Characterization for Gel State

As the clusters interconnect with each other and form a space-spanning network, the mixed suspensions show solid-like characteristics. Broadly speaking, gelation occurs, although some gels are very weak and gentle shaking of the samples is enough to destroy the gels, while other gels cannot flow by gravity. In this study, oscillatory frequency sweep and strain sweep measurements were performed on suspensions with Φ_{MS} ranging from 0.02 to 0.15, and the transitions from liquid-like to solid-like behavior triggered by Φ_{MG} were carefully identified. Gelation under the over saturated situation (which need more microgel) may intervene with jamming effect, so only the gelation due to bridging effect is considered in this study. The solid character is identified by the observation of a linear viscoelastic region with constant values of G' and G'', within which the value of G' is larger than G''. The liquid-gel state diagram in the Φ_{MS} - Φ_{MG} plane is showed in Fig. 3(a). The gray area in Fig. 3(a) indicates samples with Φ_{MS} and Φ_{MG} in that area has a yielding stress $\tau_y \geq 0.1$ Pa. The red dash line is a reference line for saturation adsorption.

Fig. 3(b) shows the typical stress dependence of storage modulus (G') inside the bridging gel regime for mixed suspensions with $\Phi_{MS} = 0.1$. When $4.3 \times 10^{-4} \leq \Phi_{MG} \leq 1.43 \times 10^{-2}$, the values of G' at the linear viscoelastic region firstly increase, and then decrease with increasing Φ_{MG}. While for samples with $\Phi_{MG} < 4.3 \times 10^{-4}$ and with Φ_{MG} slightly above 1.43×10^{-2}, no yielding behavior is observed in the experimental scale (data not shown). These phenomena indicate that the suspensions are experiencing a liquid → gel → liquid transition with increased $\Phi_{MG.}$ which could be explained by the

La Mer's theory[38, 39] of bridging flocculation. According to La Mer's description,[38,39] for a polymer-bridged colloidal suspension, the rate of bridging flocculation is proportional to $\theta(1-\theta)$ and the size of the cluster is proportional to $\theta^2(1-\theta)^2$, where θ is the surface coverage. It should be noted that the concept of surface coverage is rather imprecise since it depends greatly on the configuration of the adsorbed chains which in turn can be affected by the adsorbed amount.[56, 57] Even so, it is not surprisingly that, with the increasing concentration of bridging polymer, the maximum flocculation occurs at an intermediate dosage.

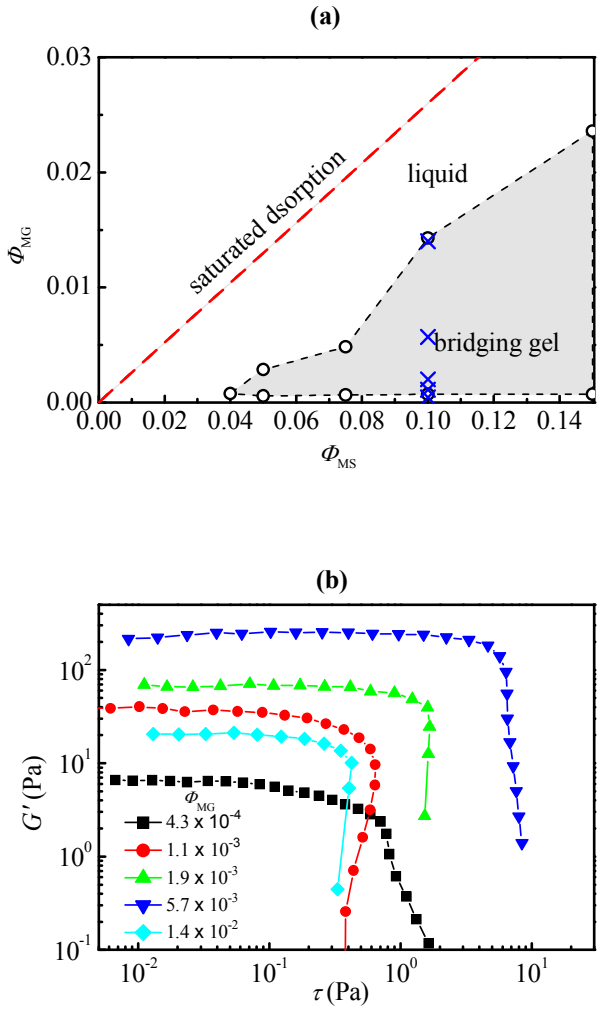

Figure 3 (a) State diagram of mixed suspensions of PS microsphere and PNIPAM microgel determined by rheological measurements; **(b)** Typical stress amplitude sweep data for mixed suspensions with Φ_{MS} = 0.1 inside the bridging gel regime, whose locations on the state diagram are marked by the blue crosses in **(a)**.

It should be noted that the criterion for rheological gel boundary is non-unified or non-critical. To clarify a sample's solid-like behavior or liquid-like behavior, one refers to the response of a sample to the given external field. For example, gel sample can be identified by the absence of flow after tube inversion. This criterion for gel is widely-used but not rigorous. Or rather, a solid-like or liquid-like response of a sample during dynamic frequency sweep measurement will depend on the set strain amplitude. The references (the given external fields or experimental conditions), is not unified in various experiments. Furthermore, the liquid to physical gel transition under rheological observation usually occurs gradually within a wide transition region. For example, in the recent paper by Laurati et al.[60] who performed a thorough study on gels formed by depletion attraction, when a gel is defined by the relaxation time of the arrested structure which is larger than the whole experimental observation time, there is a wide transition region with occurrence of attested structure but the relaxation time of the structure is inside the experimental time window. In this sense, one cannot define a critical gelation boundary through limiting rheological experiments. Here, our reference to draw the gelation boundary with τ_y = 0.1Pa on a state diagram, does not violate the criterion that the moduli G' and G'' are constant as

the function of frequency with $G' > G''$ in the experimental linear viscoelastic regime. And it does not influence our interpretation on the general shape of the state diagram.

3.3 USANS Characterization of Gel State

The modulus and yielding stress of a colloidal gel depend both on the nature and strength of the interparticle interaction and on the topology and connectivity of the gel. The information of structure and effective interaction can be extracted from the USANS data. To illustrate the model fitting, evolutions of USANS intensity obtained from mixed suspensions with $\Phi_{MS} = 0.10$ and various Φ_{MG} are shown in Fig. 4(a) as examples, where the changes in the rheological property is evident. Neutron scattering patterns are shifted vertically with each offset by a log I =1 for clarity. Symbols are experimental data points and solid lines are model fitting curves after taking into account the instrument resolution. Relatively flat curve at the low q limit indicates no macroscopic flocs in our systems, while a strong upward-sloping curve toward the low q limit corresponds to heterogeneous density distribution at large length scale. Qualitatively judging from the trends of the intensity curves, a flat → upward → flat transitions of intensities approaching to the low q limit is consistent with rheological measurements, which shows a liquid →gel → liquid transitions with increasing Φ_{MG} .

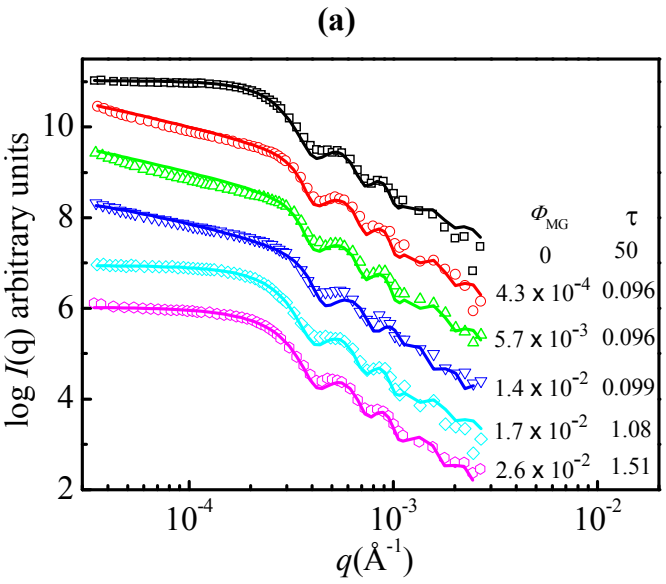

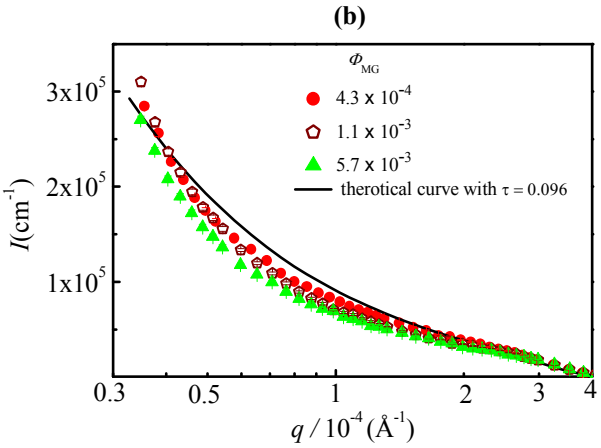

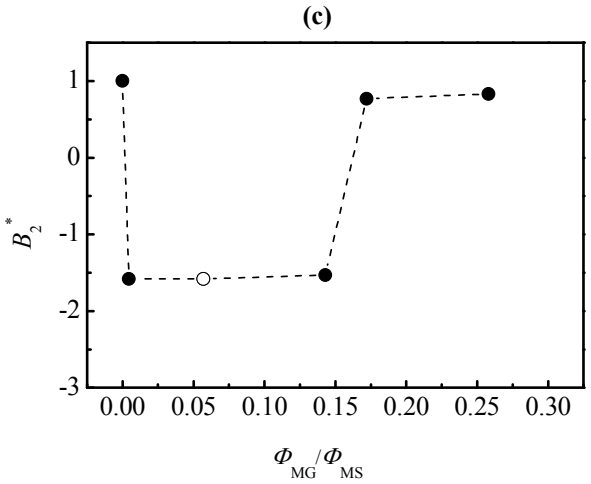

Figure 4 (a) Experimental (symbols) and fit (solid lines) intensity data scattered from suspensions with Φ_{MS} = 0.10 and various Φ_{MG}. **(b)** Comparison of model calculation with experimental scattering intensities within the range of $3.0 \times 10^{-5} < q < 3.0 \times 10^{-4}$ Å^{-1} for three gel samples with $\Phi_{MS} = 0.10$. **(c)** The corresponding reduced second virial coefficient B_2^* vs. mixing ratio (Φ_{MG}/Φ_{MS}).

In principle, the liquid theories and models are designed for liquid samples, not for gel samples, so there is no point to try to fit a curve in gel state. However, the rheological criterion for physical gel state is quite arbitrary, which is non-unified and non-critical as we mentioned above. In addition, the very weak physical gel is not in a permanent static state, but a dynamic equilibrium state. It has its own conformation structure in real space or $S(q)$ in reciprocal space. Dynamically, it should have its own $S(q,t)$ structure, the time (t) dependent part is related to the static distribution，but does not follow the simple Brownian dynamic of single particles. Based on the above consideration, we compare the data in different state to that of a curve from a liquid

theory calculation. Fig. 4(a) shows satisfactory quantitative agreement between the experimental scattering curves and the fitting curves, especially for liquid samples. However, there are slight deviations between the experimental data and fittings for samples inside the gel region, in particular at low q value ($q < 3.0 \times 10^{-4}$ Å^{-1}). Here again, within experimental accuracy, all scattering curves are in agreement with that of the bare PS microsphere dispersion in the high q region ($q > 3.0 \times 10^{-4}$ Å^{-1}). Fig. 4(b) shows the comparison of model calculation with experimental scattering intensities from three samples which show order of magnitude difference in their elasticity. According to the results of rheological measurements (Fig. 3(b)), the samples pass the liquid-solid transition boundary and form stronger gel with increasing Φ_{MG} from 4.2×10^{-4} to 5.7×10^{-3}. The theoretical curve is calculated by using the boundary value ($\tau_B = 0.096$, $B_2^* = -1.60$) on the spinodal line for Φ_{MS} = 0.10. According to Baxter *et al.*,[35] below this boundary value, samples are trapped inside the unstable region and there are no physical acceptable solutions of the PY equation. To clearly demonstrate the difference between theoretical calculation curve and experimental intensity curves, the scattering intensity in Fig. 4(b) is showed in linear scale. As compared with the theoretical curve, it is found that, there is slightly depression in experimental intensity, and the depression of intensity is relatively more significant for sample with stronger elasticity. Depression in this q region originates from the closer bonding between particles with stronger interactions. The scattering from weakest gel is more close to the theoretical curve for equilibrium-nonequilibrium transition.

The comparison of variation tendency between static scattering measurement which characterizes the equilibrium-nonequilibrium transition and rheological measurement which characterizes the liquid-solid transition, indicates that there may exist a strict rheological criterion for the liquid-solid transition meanwhile the system undergoes equilibrium-nonequilibrium transition as determining by scattering technique. That is, the nature of gel state may come from the arrested phase separation. Experimentally, the criteria do not coincide because the characteristic length scale determining the equilibrium-nonequilibrium transition and the rheological liquid-solid transition may differ significantly from each other. In the research of dynamical arrest transition in nanoparticle dispersions induced by thermoreversible adhesive interaction, Eberle *et al.*[19] have found that the scattering intensity no longer evolves but remains constant when samples are trapped inside the gel region. In their research,[19] the fits of scattering intensity of samples at gel state are indeed of the structure at the fluid phase boundary within experimental uncertainty, which confirms that gelation process is a dynamical arrest transition. Their gels have the same arrest structure at the length scales accessible by neutron measurement.

The corresponding B_2^* values extracted from the analysis of scattering data in Fig. 4(a) are plotted as a function of Φ_{MG}/Φ_{MS} in Fig. 4(c). The open circle denotes the boundary value ($\tau_B = 0.096$, $B_2^* = -1.60$) below which there are no analytical solutions. It can be seen that, the numerical values of effective B_2^* are similar for systems with various Φ_{MG} at the gleation boundaries ($\Phi_{MG} = 4.3 \times 10^{-4}$ and 1.4×10^{-2}). Moreover, these values are very close to the theoretical value for spinodal line.

Actually, for depletion systems, a connection between the gelation boundary and the spinodal line has been proposed with spinodal decomposition driving cluster formation and gelation.[7, 8, 18, 60] Evidences for gelation being a consequence of phase seperation induced by depletion attraction have been revealed for samples at relatively low concentrations.[21] PNIPAM microgel being used as a depletion agent to induce phase separation and gelation of polystyrene latex spheres has also been reported by Bayliss *et al*.[62] Our result provides evidence that, at low particle volume fraction, gelation of PS microsphere through bridging mechanism may have the same thermodynamic origins.

3.4 Mixing Ratio and Attraction Mechanism

In summary, upon increasing the strength of the effective inter-particle attraction by either bridging or depletion mechanism, the system evolves from an equilibrium liquid to a nonequilibrium, structure arrested state. Therefore, it is important to know how to control the interaction. As revealed by theoretical models[28,29] and direct measurements[30-32], the attractive strength induced by bridging polymer is very sensitive to surface coverage. Also, we know from above discussion that the effective interaction is very sensitive to mixing ratio of particles. There is a regime where the PS microspheres are sterically stabilized by the adsorbed PNIPAM microgels. Fig. 5 shows the scattering curves of mixed suspensions with various Φ_{MG}/Φ_{MS}. At Φ_{MG}/Φ_{MS} = 0.26 (Fig. 5(c)), the fit B_2^* values for these samples are all close to 1, which corresponds to a hard sphere fluid. The explanation is that the mixed

suspensions tend to achieve a saturated adsorption state at a specific mixing ratio, which have been proved in our previous studies.[40, 41, 61] In very dilute colloid suspensions, the concentration of microgel for saturated adsorption (Φ^*_{MG}) is determined by dynamic light scattering as the correlation function returned back to a narrow distributing single relaxation with increasing Φ_{MG}. In dilute colloid suspensions, Φ^*_{MG} is determined by optical microscopy observation as the minimum concentration of microgel needed to induce the disappearance of clusters of microsphere. In concentrated colloid suspensions, the Φ^*_{MG} is determined by rheological measurement as gel-liquid transition occurred with increasing Φ_{MG}. Φ^*_{MG} is found to approximately follow a linear relationship with the given Φ_{MS}. Here, $\Phi^*_{MG} = 0.26 \times \Phi_{MS}$. It should be noted that the linear coefficient is strongly dependent on the size ratio of microsphere to microgel. The approximately linear relationship between Φ^*_{MG} and Φ_{MS} indicates the adsorption of the microgel obeys Langmuir's isotherm and the equilibrium concentration of microgel remaining in the solution may be negligible after the adsorption process is completed. Here, Φ_{MG}/Φ_{MS} is the factor which can determine whether the surface of microsphere is fully covered by microgel particles or not, and hence determine that the gelation follows the bridging mechanism or the depletion mechanism.

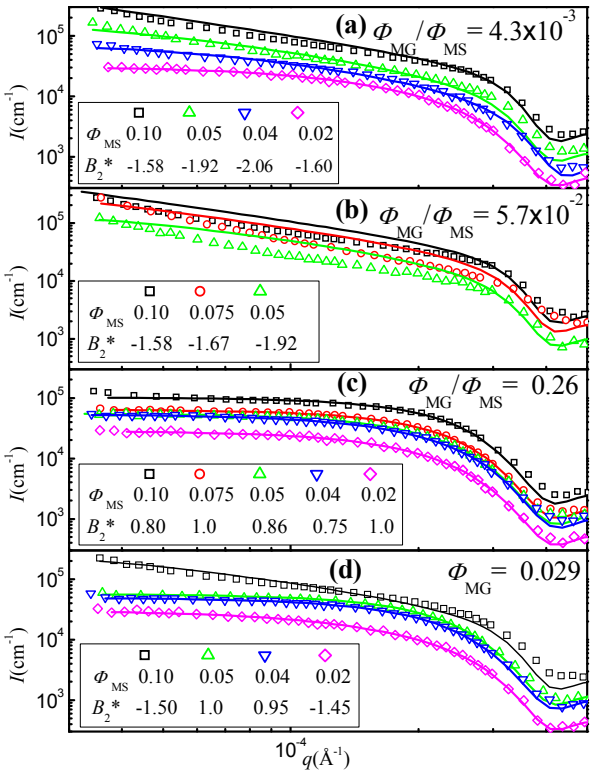

Figure 5 Experimental (symbols) and fit (solid lines) intensity data scattered from suspensions with various mixing ratios: (a) $\Phi_{MG}/\Phi_{MS} = 4.3 \times 10^{-3}$; (b) $\Phi_{MG}/\Phi_{MS} = 5.7 \times 10^{-2}$; (c) $\Phi_{MG}/\Phi_{MS} = 0.26$; (d) $\Phi_{MG} = 0.029$.

When $\Phi_{MG}/\Phi_{MS} < 0.26$, bridges between microspheres exist, and the effective inter-microsphere interaction is mainly controlled by bridging mechanism. Only a very little amount of microgels can quench systems to a state point with large attraction strength. Fig. 5(a) shows the scattering intensity from system with $\Phi_{MG}/\Phi_{MS} = 4.3 \times 10^{-3}$. In this situation, the number of small microgels is twice of the number of large microspheres. The agreement between experimental data and fitted lines are quite satisfied. The B_2^* values indicate that the systems are approaching to unstable state. When $\Phi_{MG}/\Phi_{MS} = 5.7 \times 10^{-2}$, there is evident deviation between experimental

data and theoretical calculations using the boundary values (Fig. 5(b)). In short, aggregations result from a growth process out of equilibrium.

When $\Phi_{MG}/\Phi_{MS} > 0.26$, according to the approximation that the saturated adsorption amount is about $0.26\Phi_{MS}$, there will be free microgels disperse in the suspension. Extra free microgels which are unable to adsorb to the surface of saturated large particles may generate depletion attraction. The flocculation induced by non-adsorbing polymer (here, extra free microgel) is generally referred to as depletion flocculation. The strength of effective depletion attraction depends on the free volume concentration of small particles, which is influenced by the volume fraction of large and small particles. Here the portion of microgel adsorbed on the surface of large particle should be considered, and the actual volume fraction of soft deformable microgel in dense environmental is unknown. Fig. 5(d) shows the scattering curves from mixed suspensions with the same $\Phi_{MG} = 0.029$, which is above the saturated adsorption amount for each $\Phi_{MS.}$ But the excessive value of microgel as compared to the volume fraction of large particles, $(\Phi_{MG} - 0.26\Phi_{MS})/\Phi_{MS}$, is very different for each $\Phi_{MS.}$ Although the effective strength changes in a fashion that quantitatively is not precisely known, evident attraction is observed in systems with large number of free microgel (case with $\Phi_{MS} = 0.02$) and that with less free space for microgels (case with $\Phi_{MS} = 0.10$).

4. Conclusions

When small PNIAPM microgel dispersion is mixed with the large PS microspheres

stabilized by surface coated polymers, clear transitions from bridging flocculation → stabilization → depletion flocculation are observed with an increasing concentration of microgel. The effective inter-microsphere attractions induced by either bridging or depletion of microgels are treated equally as short-ranged attraction and the interactions are characterized with USANS, despite the fact that the physical mechanisms of bridging attraction and depletion attraction are different at amolecular level. Baxter's sticky hard-sphere model is used to extract the effective inter-microsphere. The data are analyzed with Baxter's one component sticky hard-sphere model. For $\Phi_{MS} < 0.04$, system remain as liquid in all investigated concentration range of microgels. At $\Phi_{MS} \geq 0.04$, some mixed suspensions show solid-like characteristics. In this study, we are particularly interested in the behavior of samples close to the liquid-solid transition boundaries. USANS and rheological measurements allow us to deduce the static properties in the quiescent samples to their linear viscoelastic response. Three points are summarized as follows:

First, for given Φ_{MS} mixed with various Φ_{MG}, at the cases where solid-like behavior appears through bridging mechanism, the effective interaction B_2* is similar. Moreover, these B_2* values are very close to the theoretical values derived from the spinodal line. It indicates that gelation of particles in bridging flocculation system — which is often considered as a purely kinetic phenomenon especially — may be a direct consequence of equilibrium phase separation as proposed in depletion system by Lu *et al.*[21] The independence on microscopic system-specific details (bridging or depletion) implies that this conclusion should thus apply broadly to any particle

system with short-range attractions at relatively low concentrations.

Second, for gel states with given Φ_{MS}, there are order of magnitude difference in their elasticity depending on Φ_{MG}. As their scattering curves are compared with the theoretical calculation, it is found that the scattering from weakest gel is closer to the theoretical curve for equilibrium-nonequilibrium transition. It implies that there may exist a strict rheological criterion for the liquid-solid transition meanwhile the system undergoes equilibrium-nonequilibrium transition as determining by scattering technique. It is related to the questions that, what is the criterion for liquid-solid transition based on rheological measurement, and how weak can a solid (or gel) be. If the scattering curve for the experimentally onset gel state is not coincided with the theoretical curve for equilibrium-nonequilibrium transition, it may because the criterion of rheological measurement for fluid-solid transition is non-unified or non-critical.

Third, the effective interaction strength is very sensitive to mixing ratio of small to large particles. Although it changes in a way that is not quantitatively precisely known, the approximately linear relationship between the saturated adsorption concentration of microgel and the given concentration of microsphere provides a rough reference for bridging or depletion mechanism depending on whether the surface of microsphere is fully covered by microgel particles or not. Once the scenario that the bridging interaction is equal to a short-range attraction is accepted, with the simple adsorption relationship, a new state diagram of gelation and even of glass transition could be constructed, as we show in our recent paper.[61] Regarding to the interference between

two origins for ergodic to non-ergodic transition in condensed system, i.e. cage effect and bond effect, the short-ranged attractive interaction coming from the well-defined bridging bonds will help to clarify some controversies.

Acknowledgements

This work is supported by the National Basic Research Program of China (973 Program, 2012CB821503). Y. Liu acknowledges the support of cooperative agreement 70NAB10H256 from NIST, U.S. Department of Commerce. This work utilized facilities supported in part by the U.S. National Science Foundation under Agreement No. DMR-0944772. Certain commercial equipment, instruments, or materials (or suppliers, or software, …) are identified in this paper to foster understanding. Such identification does not imply recommendation or endorsement by the U.S. National Institute of Standards and Technology, nor does it imply that the materials or equipment identified are necessarily the best available for the purpose.

References

1. G. Foffi, C. De Michele, F. Sciortino and P. Tartaglia, *Phys. Rev. Lett.,* 2005, **94**, 078301.
2. V. Trappe and P. Sandkühler, *Curr. Opin. Colloid Interface Sci.,* 2004, **8**, 494-500.
3. E. Zaccarelli, *J. Phys.: Condens. Matter,* 2007, **19**, 323101.
4. P. Meakin, *Phys. Rev. Lett.,* 1983, **51**, 1119-1122.
5. E. H. A. de Hoog, W. K. Kegel, A. van Blaaderen and H. N. W. Lekkerkerker,

Phys. Rev. E, 2001, **64**, 021407.

6. J. Bibette, T. G. Mason, G. Hu and D. A. Weitz, *Phys. Rev. Lett.,* 1992, **69**, 981-984.
7. N. A. M. Verhaegh, D. Asnaghi, H. N. W. Lekkerkerker, M. Giglio and L. Cipelletti, *Physica A,* 1997, **242**, 104-118.
8. W. C. K. Poon, A. D. Pirie, M. D. Haw and P. N. Pusey, *Physica A,* 1997, **235**, 110-119.
9. S. Manley, H. M. Wyss, K. Miyazaki, J. C. Conrad, V. Trappe, L. Kaufman, D. R. Reichman and D. A. Weitz, *Phys. Rev. Lett.,* 2005, **95,** 238302.
10. F. Cardinaux, T. Gibaud, A. Stradner and P. Schurtenberger, *Phys. Rev. Lett.,* 2007, **99**, 118301.
11. S. Ramakrishnan, M. Fuchs, K. S. Schweizer and C. F. Zukoski, *J. Chem. Phys.,* 2002, **116**, 2201-2212.
12. G. Foffi, C. De Michele, F. Sciortino and P. Tartaglia, *J. Chem. Phys.,* 2005, **122**, 224903.
13. W. Götze, in *Liquids, freezing and the glass transition*, edited by J. P. Hansen, D. Levesque and J. Zinn-Justin. Amsterdam: North-Holland, 1991:287.
14. K. A. Dawson, *Curr. Opin. Colloid Interface Sci.,* 2002, **7**, 218-227.
15. P. Meakin and H. Stanley, *Phys. Rev. Lett.,* 1983, **51**, 1457-1460.
16. M. Carpineti and M. Giglio, *Phys. Rev. Lett.,* 1992, **68**, 3327-3330.
17. A. H. Krall and D. A. Weitz, *Phys. Rev. Lett.,* 1998, **80**, 778-781.
18. H. Verduin and J. K. G. Dhont, *J. Colloid Interface Sci.,* 1995, **172**, 425-437.

19. A. P. R. Eberle, R. Castañeda-Priego, J. M. Kim and N. J. Wagner, *Langmuir,* 2012, **28**, 1866-1878.

20. J. Bergenholtz, W. C. K. Poon and M. Fuchs, *Langmuir,* 2003, **19**, 4493-4503.

21. P. J. Lu, E. Zaccarelli, F. Ciulla, A. B. Schofield, F. Sciortino and D. A. Weitz, *Nature,* 2008, **453**, 499-503.

22. S. Asakura and F. Oosawa, *J. Chem. Phys.,* 1954, **22**, 1255-1256.

23. G. J. Fleer and J. M. H. M. Scheutjens, ACS Symp. Ser., 1984, **240**, 245-263.

24. E. Dickinson and L. Eriksson, *Adv. Colloid Interface Sci.,* 1991, **34**, 1-29.

25. E. Dickinson, *J. Colloid Interface Sci.,* 1989, **132**, 274-278.

26. E. Dickinson, *J. Chem. Soc., Faraday Trans.,* 1990, **86**, 439-440.

27. E. Dickinson, *J. Chem. Soc., Faraday Trans.,* 1995, **91**, 4413-4417.

28. J. Klein and P. Pincus, *Macromolecules,* 1982, **15**, 1129-1135.

29. G. J. Fleer, J. M. H. M. Scheutjens and M. A. C. Stuart, *Colloids Surf., A,* 1988, **31**, 1-29.

30. J. N. Israelachvili, M. Tirrell, J. Klein，Jacob and Y. Almog, *Macromolecules,* 1984, **17**, 204-209.

31. J. Klein and P. F. Luckham, *Nature,* 1984, **308**, 836-837.

32. S. S. Patel and M. Tirrell, *Annu. Rev. Phys. Chem.,* 1989, **40**, 597-635.

33. R. J. Baxter, *J. Chem. Phys.,* 1968, **49**, 2770-2774.

34. W. G. T. Kranendonk and D. Frenkel, *Mol. Phys.,* 1988, **64**, 403-424.

35. R. O. Watts, D. Henderson and R. J. Baxter, *Adv. Chem. Phys.,* 1971, **21**, 421-430.

36. Y. C. Chiew and E. D. Glandt, *J. Phys. A: Math. Gen.,* 1983, **16**, 2599-2608.

37. B. Bharti, J. Meissner, S. H. L. Klapp and G. H. Findenegg, *Soft Matter,* 2014, **10**, 718-728.

38. R. H. Smellie Jr and V. K. La Mer, *J. Colloid Sci.,* 1958, **13**, 589-599.

39. V. K. La Mer, *Discuss. Faraday Soc.,* 1966, **42**, 248-254.

40. C. Zhao, G. Yuan and C. C. Han, *Macromolecules,* 2012, **45**, 9468-9474.

41. C. Zhao, G. Yuan, D. Jia and C. C. Han, *Soft Matter,* 2012, **8**, 7036-7043.

42. A. T. J. M. Woutersen, R. P. May and C. G. de Kruif, *J. Colloid Interface Sci.,* 1992, **151**, 410-420.

43. A. Vrij, M. H. G. M. Penders, P. W. Rouw, C. G. de Kruif, J. K. G. Dhont, C. Smits and H. N. W. Lekkerkerker, *Faraday Discuss. Chem. Soc.,* 1990, **90**, 31-40.

44. A. Malijevsky, S. B. Yuste and A. Santos, *J. Chem. Phys.,* 2006, **125**, 074507.

45. N. E. Valadez-Perez, A. L. Benavides, E. Scholl-Paschinger and R. Castaneda-Priego, *J. Chem. Phys.,* 2012, **137**, 084905.

46. M. G. Noro and D. Frenkel, *J. Chem. Phys.,* 2000, **113**, 2941-2944.

47. H. Senff and W. Richtering, *J. Chem. Phys.,* 1999, **111**, 1705-1711.

48. G. K. Batchelor, *J.Fluid Mech.,* 1977, **83**, 97-117.

49. J. G. Barker, C. J. Glinka, J. J. Moyer, M. H. Kim, A. R. Drews and M. Agamalian, *J. Appl. Crystallogr.,* 2005, **38**, 1004-1011.

50. S. R. Kline, *J. Appl. Crystallogr.,* 2006, **39**, 895-900.

51. K. Wong, B. Cabane and R. Duplessix, *J. Colloid Interface Sci.,* 1988, **123**, 466-481.

52. B. Cabane, K. Wong, T. K. Wang, F. Lafuma and R. Duplessix, *Colloid Polym. Sci.,* 1988, **266**, 101-104.

53. L. S. Ornstein and F. Zernike, *Proc. Acad. Sci.*, 1914, **17**, 793-806.

54. J. K. Percus and G. J. Yevick, *Phys. Rev.,* 1958, **110**, 1-13.

55. A. T. J. M. Woutersen, R. P. May and C. G. De Kruif, *J. Colloid Interface Sci.,* 1992, **151**, 410-420.

56. J. Gregory and S. Barany, *Adv. Colloid Interface Sci.,* 2011, **169**, 1-12.

57. J. Gregory, *Colloids Surf., A,* 1988, **31**, 231-253.

58. P. D. Kaplan, J. L. Rouke, A. G. Yodh and D. J. Pine, *Phys.Rev. Lett.,* 1994, **72**, 582-585.

59. G. J. Fleer, M. A. Cohen-Stuart, J. M. H. M. Scheutjens, T. Cosgrove and B. Vincent, *Polymer at interface*, London: Chapman & Hall; 1993.

60. M. Laurati, G. Petekidis, N. Koumakis, F. Cardinaux, A. B. Schofield, J. M. Brader, M. Fuchs and S. U. Egelhaaf, *J. Chem. Phys.* 2009, **130**, 134907-134920.

61. C. Zhao, G. Yuan and C. C. Han, *Soft Matter,* 2014, **10**, 8905 - 8912.

62. K. Bayliss, J. S. van Duijneveldt, M. A. Faers and A. W. P. Vermeer, *Soft Matter,* 2011, **7**, 10345-10352.